

# Wireless Controlled Robotic Hand using an LED-LDR Sensor

## Amer Alsaraira

Biomedical Engineering Department, School of Applied Medical Sciences, German Jordanian University, Amman, Jordan  
amer.alsaraira@gju.edu.jo (corresponding author)

## Khaleel Younes

Biomedical Engineering Department, School of Applied Medical Sciences, German Jordanian University, Amman, Jordan  
k.younes@gju.edu.jo

## Samer Alabed

Biomedical Engineering Department, School of Applied Medical Sciences, German Jordanian University, Amman, Jordan  
samer.alabed@gju.edu.jo

## Omar Saraereh

Department of Electrical Engineering, Faculty of Engineering, The Hashemite University, Zarqa, Jordan  
eloas2@hu.edu.jo

Received: 25 July 2024 | Revised: 7 August 2024 | Accepted: 18 August 2024

Licensed under a CC-BY 4.0 license | Copyright (c) by the authors | DOI: <https://doi.org/10.48084/etasr.8507>

## ABSTRACT

The goal of this study is to develop a wireless-controlled robotic hand that is capable of replicating the movements of a human hand. A central objective of the design process is the development of a sensing technique that can accurately capture and translate human hand movements into electrical signals in a sustainable manner. This sensing technology relies on the detection of flexion and extension in the human hand, achieved through the modulation of light transmitted from a Light-Emitting Diode (LED) and received by a Light-Dependent Resistor (LDR). Five sensors, each corresponding to a finger, are integrated into a glove worn by the user, thereby enabling an intuitive control of the robotic hand. The sensors generate discrete electrical signals with each finger movement, which are then wirelessly transmitted via nRF24l01 modules to the microcontroller of the robotic hand. Subsequently, the microcontroller generates the requisite electrical signals to actuate the servo motors, thereby orchestrating the movement of the robotic fingers to mimic human hand gestures. The robotic hand, comprising 46 individual components fabricated using biodegradable polylactic acid material via 3D printing, successfully achieves its objective of replicating human hand movements. However, a minor delay in milliseconds is observed between human hand movements and the corresponding robotic hand movements. Despite this delay, the developed system shows promise for applications in hazardous environments, such as dangerous chemistry experiments, and enhances safety in the medical laboratory. It may also play a crucial role in remote surgery procedures.

*Keywords-robotic hand; microcontroller; hazardous environments; sustainable developmen; safety; sensing technique*

## I. INTRODUCTION

It is widely accepted that individuals may face significant risks when undertaking tasks in close proximity to sources of potential danger. For example, working in factories with elevated temperatures can result in a range of physiological effects, including an increase in platelet and red cell count,

blood viscosity, and plasma cholesterol levels during heat stress. Additionally, there is an elevated risk of mortality from coronary and cerebral thrombosis. Healthcare workers in hospitals may also experience adverse effects on their health and quality of life due to the exposure to hazardous chemicals related to their occupation. The extent of this exposure can vary significantly depending on the specific clinical unit and job role

[3, 4]. Furthermore, exposure to hazardous chemicals has resulted in damage to the nervous, hematopoietic, or reproductive systems [5]. These issues demand tangible solutions and have been the subject of considerable research. Some of the solutions included the design of a robotic hand that simulates remote human hand movements, with a primary focus on the method used for capturing hand movements. Some of these solutions employed Electromyographic signals (EMG) to capture electrical signals from muscles [6-8]. Another group of researchers used high-speed cameras to capture a substantial number of images of the human hand. The images were transmitted to the robotic hand, which, in turn, moved its fingers based on the positions captured in the images [9]. Another methodology deployed by researchers entailed the placement of flex sensors on the human hand's fingers for the purpose of capturing finger movements, subsequently translating them into electrical signals and transmitting them to the robotic hand [10-16].

It is apparent that the field of hand motion sensing encompasses a range of technological approaches. The primary objective of this work is to introduce a novel sensing technique that has not previously been used in this field for the detection of finger movements at a relatively low cost. This innovation provides users with multiple options, offers complementary capabilities, and has the potential to enhance the overall performance of the system. This study presents an innovative sensing technology that employs LEDs and LDRs positioned in opposing directions within a hollow black wire. The intensity of the light received by the LDR is inversely proportional to the degree of finger flexion, resulting in corresponding alterations in the LDR values. The fluctuations in LDR values enable the identification of finger movements. This method is analogous to the technique outlined by authors in [17] although its implementation differs. In order to model an infrared-based identification system, infrared LED arrays were utilized as a transmitter and IR photodiodes were used as a receiver. It is presumed that surgical robots, operated via handheld devices, will continue to be a fundamental aspect of enabling remote surgical procedures in the future. The prevailing surgical robotic system is typically composed of mechanical and camera arms. Some mechanical arms are responsible for handling surgical instruments, while others are tasked with performing surgical procedures within the human body. The camera arm is responsible for capturing patient information and transmitting it to a computer console, thereby enabling the surgeon to monitor the patient. The surgeon is able to manipulate the robotic hands to various positions. Even though surgical robots are an indispensable tool in the operating room, the cost of the hardware and software required for robotic surgery is often prohibitive, making it inaccessible for many surgical procedures [18]. The development of a wireless-controlled robotic hand that mimics human hand movement represents a significant advancement in robotics and human-computer interaction. The ability to replicate the human hand's gestures is a notable achievement. The system employs the use of LEDs and LDRs to facilitate the detection of finger movements, with the integration of five sensors within a glove for the purpose of intuitive control. The sensors transmit electrical signals via NRF24101 modules to a microcontroller, which activates the

servo. The robotic hand, constructed from 46 biodegradable PLA components, is integrated with servo mechanisms that enable it to move in a manner that closely resembles human hand movements.

The system displays considerable prospective for use, in hazardous environments, including dangerous chemistry experiments and medical laboratories. Furthermore, it has the potential to markedly enhance remote surgical procedures. Furthermore, the robotic hand could be employed in disaster response scenarios, enabling operators to undertake delicate tasks remotely in unsafe conditions. Additionally, the particular technology has the potential to be used in the context of space exploration, where it could facilitate the performance of tasks in the vacuum of space or on other planetary bodies by astronauts. Moreover, the specific technology could prove advantageous in manufacturing and assembly lines, enhancing precision and safety in handling delicate components. This paper presents a comprehensive investigation of a robotic hand system, which is divided into distinct sections that provide detailed information on its architectural framework, materials, components, methods, empirical results, and implications. Additionally, the present study provides a clear depiction of the system's structure through a block diagram, thus facilitating understanding of its design. Furthermore, it comprises a detailed examination of the materials employed and the construction techniques used, elucidating the technical complexities inherent to the system's development. The empirical results of the investigation, including the LDR readings, performance in darkness, time delay analysis, and robotic hand movement, are presented. These results provide tangible evidence of the system's functionality, presenting a critical analysis, which offers insights into the system's strengths, limitations, and potential for improvement. The paper concludes by emphasizing the practical applications of the developed system, particularly its relevance regarding individuals working in hazardous environments and disabled individuals in their daily lives. This underscores the potential societal impact of the system.

## II. BLOCK DIAGRAM

The objective of the proposed system is to replicate the complex movements of a user's hand with a high degree of precision. This objective is accomplished through the implementation of a precisely designed operational configuration, which is shown in the block diagram displayed in Figure 1. The operational setup is centered upon LDRs, which are responsible for detecting the subtle positional changes in the user's hand. Afterwards, the LDR readings are analyzed by a microcontroller, which converts them into an electrical signal that can be interpreted as a representation of the hand's movement. The signal is transmitted via a specialized transmitter to a receiver that is prepared to receive the data, traversing a specific communication channel. Upon reception, another microcontroller interprets the signal, subsequently directing the servo motors to move the robotic hand in precise degrees corresponding to the LDR readings. This process ensures the accurate reproduction of human hand movements, thereby guaranteeing the faithful replication of human hand movements.

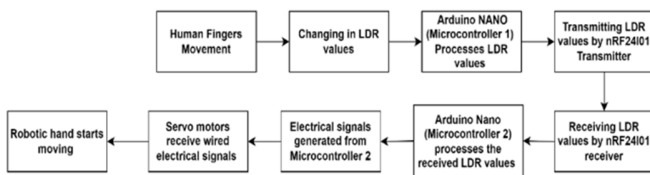


Fig. 1. The block diagram of the system.

### III. MATERIALS AND METHODS

#### A. List of Components

In order to meet the specified criteria, including cost-effectiveness, enhanced accuracy, affordability, and reliability, it was essential to conduct a thorough selection process for the system components. Moreover, the system was required to accommodate the integration of multiple sensors. Accordingly, a design comprising two discrete components—a glove and a 3D-printed robotic hand—was developed to satisfy the following criteria:

- **Wireless modules:** two NRF24L01 transceiver modules were deployed, functioning in a dual capacity as both transmitter and receiver within the system. This configuration enabled the creation of a variety of applications. The use of the NRF24L01 module ensured the reliability of data communication, thereby preserving the integrity of the transmitted data upon reception. Operating within the universally accepted Industrial, Scientific, and Medical (ISM) frequency band spanning 2,400-2,483.5 GHz, this module boasts an impressive transmission range of up to 1 km, thus providing an effective solution for extensive data transmission requirements.
- **Arduino nano:** two Arduino Nano boards were deployed, with the one serving the function of controlling the master glove and the other managing the robotic hand. The Arduino Nano, noted for its compact dimensions and compatibility with breadboards, operates within a voltage range of 0 to 5 volts. The device features 14 digital pins that can be configured as inputs or outputs, as well as 6 Pulse Width Modulation (PWM) pins. Each digital and analog pin can be utilized to fulfill a variety of functions. However, the primary objective of this study was to configure them as either input or output.
- **LED technology:** in the proposed system, five blue LEDs were put into service, with each LED designated for a specific finger. The blue LEDs employ a silicon carbide semiconductor material and emit light within the wavelength range of 403 nm to 505 nm. It is noteworthy that these light-emitting diodes possess a threshold voltage of 3.6 volts.
- **Fixed resistors and LDRs:** five 220-ohm resistors were used to safeguard each LED. Furthermore, a second set of five 220-ohm resistors was employed, with each of them being connected in series with each LDR, thus establishing a voltage divider circuit.
- **Servo motors:** the SG90 servo motors, which operate at 5 V, were employed as actuators in the system. The motors permitted a controlled rotation of up to 180 degrees. The

principal function of these components was to facilitate the movement of the model.

- **Power supplies:** given that the system is composed of two principal components, namely the master glove and the robotic hand, it is necessary to have two power supplies. The prototype primarily utilizes two 9-volt lithium batteries for power.

#### B. Master Glove and Sensing Technique

The fundamental premise of the work is to achieve an exact replication of the user's finger movements by the robotic hand. In order to achieve this, the user is required to wear a glove known as the Master Glove. The Master Glove comprises three principal components: the sensing element, the control apparatus, and the transmitter module. The sensing technique is of critical importance, as it determines the accuracy and sensitivity of the system. To achieve optimal results, a specialized sensor was developed and designed to detect the movements of the fingers. The sensor's operational principle is based on the quantity of the light absorbed. To this end, a black wire was procured and hollowed out from the interior, leaving both sides open. An LED was securely affixed to one side of the wire in a manner that prevented any light from escaping. On the opposite side of the sensor, along the path of the LED's emitted light, an LDR was placed in accordance with the specifications evidenced in Figure 2. The resistance of the LDR is inversely proportional to the amount of the light received from the light emitter [20]. Then, both sides were sealed with silicone in order to prevent light leakage from the black wire.

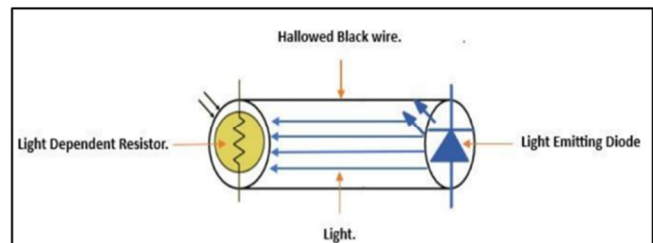


Fig. 2. The concept of the sensor.

As depicted in Figure 3, the sensor was integrated into each finger of the Master Glove. When the finger is fully extended, the sensor is also fully extended. Consequently, the LDR is exposed to the maximum level of light, as it is positioned directly in front of the LED. Therefore, the LDR reading reaches its minimum point. The amount of light received by the LDR will gradually decrease with each finger flexing motion. This is due to the light undergoing scattering within the wire, which diminishes its energy. Hence, only a minor proportion of the light reaches the light-dependent resistor, as presented in Figure 4. This results in an incremental increase in the resistor's resistance value as the flexing angle rises, due to the diminished amount of light reaching it. In order to ascertain the values of each LDR on each finger, a fixed resistor was connected in series with each LDR, along with a Direct Current (DC) voltage of 5 volts. This configuration resulted in the formation of a voltage divider circuit. The output voltage

across the LDR was quantified using an Arduino Nano microcontroller, as portrayed in the sensing circuit, in Figure 5.



Fig. 3. The master glove.

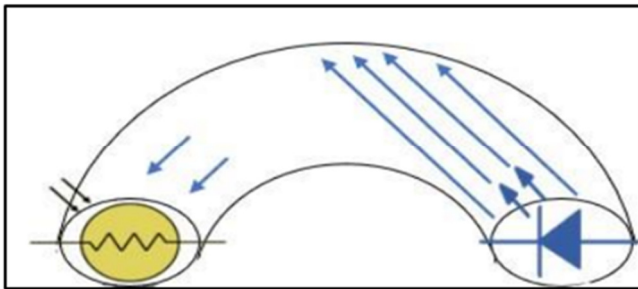


Fig. 4. The amount of light when the sensor is flexed.

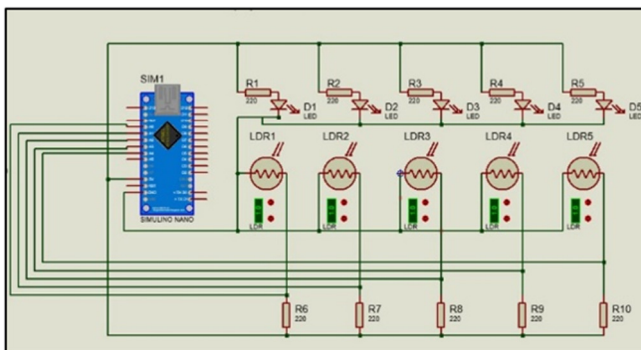


Fig. 5. The schematic diagram of the sensing circuit.

Given the known input voltage, output voltage, and the value of the fixed resistor, the value of the LDR could be calculated as:

$$LDR = \frac{V_{out} \times \text{Fixed Resistor}}{V_{in} - V_{out}} \quad (1)$$

C. Transmitter pins connection

The voltage values read by the Arduino will be converted into electrical resistance values using the specified equation. These converted values will be then used to transmit wireless electrical signals to the robotic hand controller, contingent upon the aforementioned resistance values. To transmit these electrical signals to the robotic hand, an extensive research project was undertaken, resulting in the selection of the nRF24L01 wireless communication module. The transmitter is equipped with eight male pins, which were connected in accordance with the specifications outlined in the data sheet, as illustrated in Table I. These include the Ground pin (GND), the Voltage Common Collector pin (VCC), the Chip Enable pin (CE), the Chip Select Not pin (CSN), the Serial Clock pin (SCK), the Master Out Slave In pin (MOSI), the Master in Slave Out pin (MISO), and the Interrupt Request pin (IRQ). The transmitter operates via a Serial Peripheral Interface (SPI), necessitating correct connection to the microcontroller (i.e., the SPI pins on the microcontroller) for optimal functionality. It is necessary to connect the SCK, MOSI, and MISO pins to the corresponding pins on the Arduino. The relevant pins are D13, D11, and D12. The CE and CSN pins may be connected to any digital pins of the Arduino [21]. In order to facilitate communication with the transceiver, the SPI and the RF24 library were incorporated into the Arduino program code.

TABLE I. NRF24L01 TRANSMITTER TO ARDUINO NANO PINS CONNECTION

nRF2401 Transmitter Pins	Arduino Nano Pins
CE	D9
CSN	D10
SCK	D13
MOSI	D11
MISO	D12
VCC	+5V
GND	COM/GND

D. Robotic Hand and Actuating System

The design files for the printed hand were accessible on the website and were manufactured using white biodegradable PLA material, selected for its low printing temperature and smooth surface [22]. The arm was constructed from 46 discrete components, produced via 3D printing, all of which required sanding to achieve the desired polished texture. Each digit was equipped with three rotational joints. Prior to the application of an adhesive to the joints and tips, two distinct wire types were threaded through the fingers. One wire, which resembled a tendon, was composed of braided fishing line, while the other was a rubber robe that was used to provide a pulling force for finger extension, thus enabling the hand to open. The mechanism involved the knotting of the rubber rope at the finger's tip on two occasions, with the fishing line subsequently used to secure it. An adhesive was applied with the objective of concealing the knots and bonding the fingertips. Stainless steel wires of varying diameters (1 mm and 2 mm) were utilized to connect the three rotational joints, with the thicker 2 mm wire reserved for larger fingers, such as the middle finger and

thumb. The application of an adhesive was of great importance in maintaining the structural integrity of the fingers and preventing their disintegration. Once the printing of the components was complete, the initial stage of the assembly process involved the construction of the palm with the wrist, which serves as the fundamental structure of the arm. The assembly process was conducted using three M6 bolts, with a diameter of 6 mm and a length of 80 mm. In particular, a single bolt was employed to secure the thumb to the palm, while a second bolt facilitated the connection between the wrist and the palm. The final bolt was used to affix the inferior portion of the palm to the superior half.

The adhesive was applied along with a nut to ensure stability and to prevent the wrist from moving under applied force. Once the adhesive was completely dry and it was confirmed that all fingers were functioning properly, the next step was to connect the forearm to the wrist, as shown in the complete system in Figure 6. This required adding two additional components to the model and making minor adjustments to accommodate unnecessary filament remnants while creating more space to house the model's electronics. Once these adjustments were made and the additional parts dried, the motor housing could be positioned on the model along with the motors themselves.

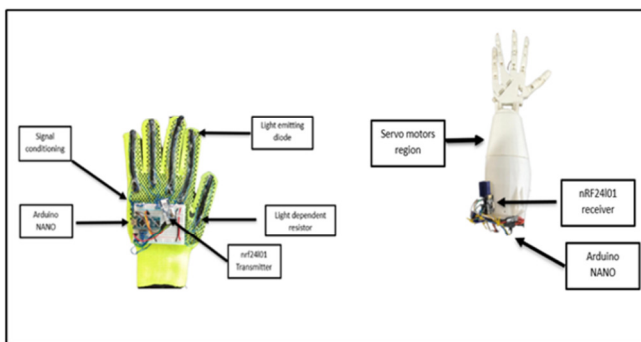


Fig. 6. Complete master glove and complete robotic hand.

### E. Receiver Pins Connections

Once the signal is transmitted from the master glove, it is received by the nRF24L01 module. This module is then connected to the microcontroller of the robotic hand, as evidenced in Table II, with each pin from the receiver being connected to a specific pin on the microcontroller.

### F. Actuating Circuit

When the electrical signal has been transmitted from the Master Glove and received by the robotic hand, the controller then proceeds to send wired electrical signals to the servo motors. The VCC and ground connections were made to each servo, with each servo being connected to a different analog pin (A0 to A4), as observed in Figure 7. The objective of these signals is to reproduce the movements of the Master Glove's hand in accordance with the sensor readings that have been received. The capacity of the controller to regulate electrical impulses enables precise control over the servo motors, allowing them to exert tension on the connected wires. As the

motors execute the commanded rotations to the specified angles, the wires are drawn or released in accordance with the requisite movements, thereby enabling the fingers of the robotic hand to imitate the actions of the Master Glove's wearer. The controller acts as an intermediary between the sensor readings and the servo motors, enabling the robotic hand to replicate the intricate movements of the Master Glove. The precise control of the servo actuators allows accurate and synchronized motion, thereby ensuring that the robotic hand closely mimics the actions conducted by the Master Glove user. This integrated system of signal transmission, reception, and control is of vital importance in achieving the desired functionality of the robotic hand, as it enables the replication of the user's hand movements in real time.

TABLE II. NRF24L01 RECEIVER TO ARDUINO NANO PINS CONNECTION

nRF2401 Receiver Pins	Arduino Nano Pins
CE	D9
CSN	D10
SCK	D13
MOSI	D11
MISO	D12
VCC	+5V
GND	COM/GND

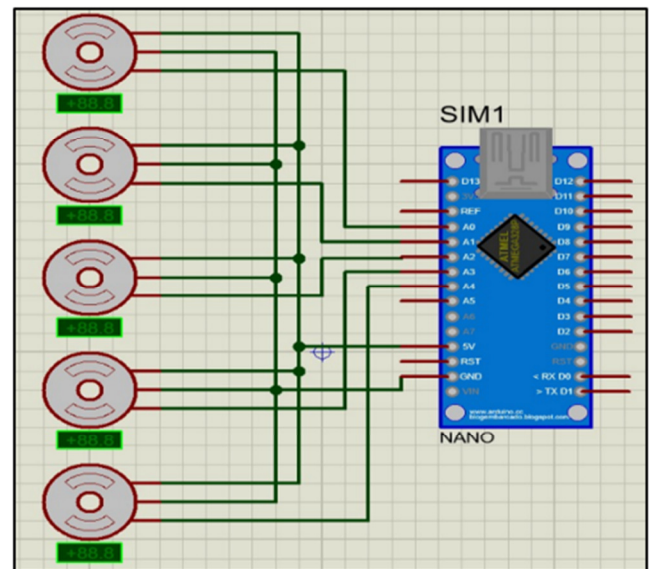


Fig. 7. The schematic diagram of the actuating circuit.

### G. Programming and Flowcharts

In consideration of the two discrete systems comprising the transmitter and receiver components, a dual set of flowcharts has been developed, as shown in Figure 8. The initial focus is on the transmitter flowchart, which pertains to the transmitter facet. Its initiation is marked by the inclusion of the nRF library, which is specialized and aligned with the wireless module in use. The flowchart entails the declaration of five distinct variables, each corresponding to the five fingers under consideration. In a methodical approach, the analog pins, spanning from A0 to A4, are designated as input interfaces. The iterative loop assumes the crucial task of measurement. In

this loop, the voltages obtained from the analog pins are converted into LDR values through the implementation of the voltage divider equation.

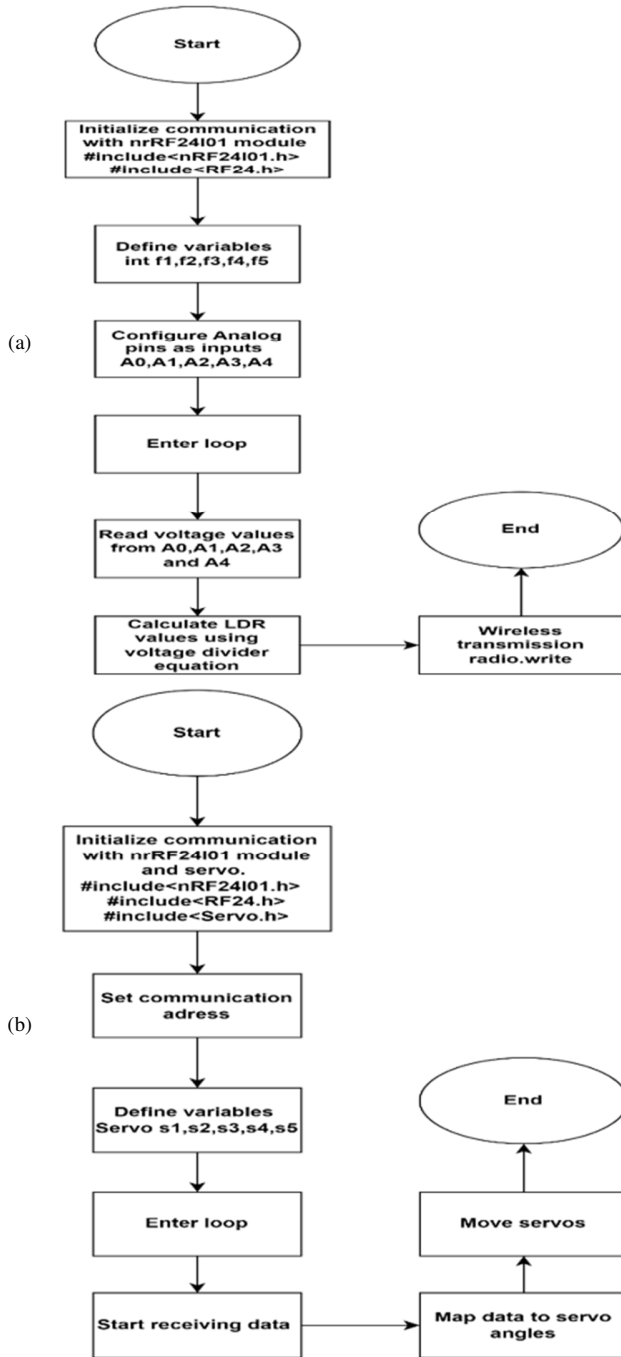


Fig. 8. Flowchart of the processing in the (a) master controller and (b) slave controller.

The final stage of this process is the transmission of the resulting analog data to the microcontroller located within the robotic hand. This is achieved through the use of the radio.write code. This methodical approach guarantees

the uninterrupted transfer of essential sensory data from the transmitter component to the receiver module. With regard to the receiver component, which corresponds to the robotic hand in this scenario, the flowchart showcased in Figure 8 (b) commences with the initiation of new library declarations. In particular, two pivotal libraries are introduced: one for the nRF receiver module and another for servomotor control. Communication addresses are declared in order to establish a reliable connection between the transmitter and receiver. The flowchart defines five distinct variables, each assigned to a corresponding servomotor unit, thereby ascertaining precise control over the movements of the robotic hand, while addressing the task of receiving data, which is carried out within a loop structure. During this phase, the system reads the unprocessed input from the transmitter. Mapping procedures are employed to transform the aforementioned raw data values into precise positional commands for the servomotors, which guarantees that the input range from the LDRs is proportionately converted to the output range required by the servomotors, thus enabling accurate and responsive control. The mapped values are then transmitted to the respective servomotor units, which cause movements that vary based on the LDR values received from the transmitter. This process enables the precise and synchronized movements of the robotic hand, which reflect the intended actions based on the LDR values.

#### IV. RESULTS

##### A. LDR Values in Three Different Positions

This section concentrates on the values of the LDRs. Readings were obtained for each light-dependent resistor in each finger, in three distinct positions. The initial position was that of the hand in a fully extended state, with all fingers in a fully extended position. The readings were recorded for a specified duration, as exhibited in Figure 9. Furthermore, the procedure was repeated with the fingers in a half-way flexed position and a fully flexed position, as shown in Figures 10 and 11, respectively. It should be noted that all readings were taken under normal room lighting conditions.

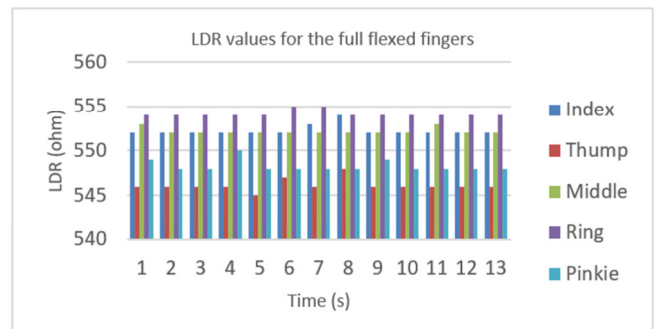


Fig. 9. LDR values for the full extended fingers.

##### B. Darkness Test

In the preceding results, all measurements were conducted under standard room lighting conditions, which were selected as the baseline for comparison. However, in this section, the

LDR values were measured in a completely darkened room to examine the impact of ambient light on the sensor. Following the measurement of LDR values in three positions (fully extended, halfway flexed, and fully flexed) with great precision, it was observed that the readings in the dark environment remained consistent with those obtained under normal lighting conditions.

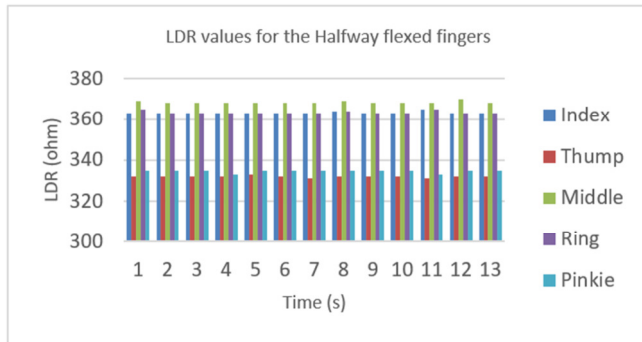


Fig. 10. LDR values for the halfway flexed fingers.

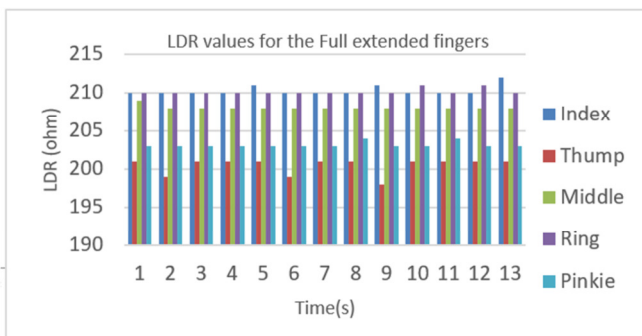


Fig. 11. LDR values for the full flexed fingers.

### C. Time Delay Test

The objective of this experiment was to ascertain the temporal discrepancy between the movement of the human hand and the corresponding movement of the robotic hand, with a particular emphasis on the individual fingers, as illustrated in Figure 12. To quantify this interval, a stopwatch was used. The stopwatch was initiated at the moment of complete closure of the human finger and ceased at the moment of full closure of the corresponding finger on the robotic hand. This procedure was repeated for each finger individually. To isolate the movement of each finger and prevent unintentional activation of other fingers, all four wires of the servo were disconnected from the microcontroller between trials. This precautionary measure was taken due to the inherent difficulty in moving certain fingers independently, such as the pinkie finger, which may inadvertently trigger movement in other fingers of the robotic hand. The objective was to accurately measure the delay between human and robotic finger movements by sequentially focusing on each finger in isolation. It is noteworthy that the process was repeated 10 times for each finger, and after that, the mean delay was calculated. This iterative approach was deployed to mitigate the

effects of variability and to ensure a more representative estimation of the delay between human and robotic finger movements.

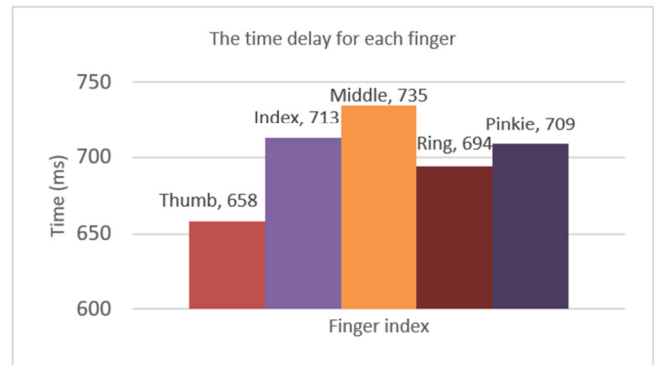


Fig. 12. The time delay between each human finger movement and each corresponding robotic finger movement.

### D. Movement of the Robotic Hand

In its initial operational phase, the robotic hand demonstrated effective functionality in both opening and closing motions, accurately replicating human hand movements in closing and opening. Additionally, it exhibited successful object-picking capabilities, reproducing the human hand's movement patterns, as shown in Figure 13. However, following repeated cycles of opening and closing, the robotic fingers demonstrated a gradual decline in their ability to return to their fully extended position with precision, as initially observed. Some fingers reached only halfway, while others approached full extension but failed to reach it optimally. Conversely, during the closing motion, all fingers displayed consistent and effective closure, even after numerous repetitions.



Fig. 13. The robotic hand picking up an object in a manner that closely resembles the human hand.

## V. DISCUSSION

The sensors demonstrated the ability to effectively detect both the flexion and extension of human hand movements, converting them into electrical signals. This fulfills the primary objective of sensors, which is to convert various forms of energy into electrical signals. When the fingers were fully extended, the LDRs received the greatest light intensity, as they

were positioned directly in front of the LEDs. Consequently, the LDR values exhibited their lowest readings, with an average of 200.46 ohms for the thumb, 210.07 ohms for the index finger, 208.07 ohms for the middle finger, 210.15 ohms for the ring finger, and 203.16 ohms for the pinky finger. In contrast, when the fingers were flexed to a position halfway between the fully extended position and the fully flexed position, the amount of light reaching the LDR was decreased due to the scattering and attenuation of light within the wire. This resulted in a reduction in the LDR values in comparison to the fully extended position. As the fingers were flexed, the amount of light reaching the LDR decreased, leading to a corresponding decrease in the LDR values. The mean LDR readings were 331.92 ohms for the thumb, 363.20 ohms for the index finger, 368.31 ohms for the middle finger, 363.3 ohms for the ring finger, and 343.6 ohms for the pinky finger. Upon full flexion of the finger, the LDR reached its highest values. This is due to the fact that no further light was able to reach the LDR in this position, which resulted in higher resistance readings. The mean resistance value was determined to be 546.15 ohms for the thumb, 552.20 ohms for the index finger, 552.15 ohms for the middle finger, 554.15 ohms for the ring finger, and 548.3 ohms for the little finger. Moreover, it was noted that the sensor performance and LDR readings remained unvaried, exhibiting no deviation whether under normal room lighting conditions or in complete darkness. This constancy indicates that LDRs were effectively shielded within the black wire, hence ensuring minimal exposure to external light sources. Therefore, the only source of illumination was the LEDs. A discernible time delay between the movement of each human finger and the corresponding action of the robotic fingers, can be attributed to a number of factors, including the operation of the wireless module.

It is inevitable that data transmission from the transmitter to the receiver will introduce a time delay, which is referred to as the transmission time. This delay is further compounded by the processing time required by the two microcontrollers, which must analyze the incoming data and send appropriate instructions to the servo motors. The transmission time is contingent upon the distance between the transmitter and the receiver, as well as the medium through which the signal traverses. Furthermore, the processing time of the microcontrollers is dependent upon their computational speed and the complexity of the data being processed. This cumulative delay affects the overall system performance, making it essential to optimize both transmission and processing times to ensure efficient and timely communication between the transmitter, microcontrollers, and servo motors. It is, however, noteworthy that the observed delay measured in milliseconds, was minimal. In the future, the potential adoption of 5G communication technology and the use of high-speed microcontrollers may result in further improvements, including a reduction in time delays. Regarding the movement of the robotic hand, it was observed that the device demonstrated effective operation during both opening and closing actions. These actions were found to successfully imitate the movements of a human hand and to grasp objects in a manner that was both dexterous and precise. However, as previously stated, following a considerable number of repetitions of

opening and closing, the robotic fingers encountered difficulty in returning to their fully extended position. This issue originated from the rubber robe, which was responsible for retracting the fingers to their fully extended state, becoming stretched and elongated to a degree that exceeded its elastic limit, and entering the plastic region. As a result, it was no longer able to serve as a rubber component capable of retracting the fingers. To address this issue, it is recommended that higher-quality rubber materials be used to certify the longevity and efficacy of the retracting mechanism.

## VI. CONCLUSIONS

The study presents a notable advancement in the sustainable development of a wireless-controlled robotic hand system that effectively emulates human hand movements. Notable achievements include the successful construction of the robotic hand, the incorporation of sensing technology to capture human hand movements, and the translation of these movements into electrical signals using Light-Dependent Resistors (LDRs). The system's capacity to function accurately in the presence of varying ambient light conditions is noteworthy, exemplifying its resilience and adaptability. However, the observed time delay in finger movement, ranging from 698 ms to 735 ms, represents a significant limitation for potential industrial applications. To address this challenge, the integration of higher-speed data transmission technologies, such as 5G, may be necessary.

Although the robotic hand accurately replicates human hand movements during opening and closing, issues emerged with regard to the return of the fingers to their fully extended position over time. This was attributed to the quality of the rubber components used. To further optimize performance, the study suggests implementing a more sophisticated robotic hand design and utilizing higher-quality rubber materials. In conclusion, the research represents a significant advancement in the field of robotics, demonstrating the potential for the creation of lifelike robotic systems capable of performing intricate tasks. Future research could concentrate on enhancing speed and precision while guaranteeing durability and dependability in diverse operational settings, thereby benefiting individuals engaged in hazardous occupations and disabled individuals in their daily activities. Furthermore, by concentrating on the degrees of freedom in finger movements, this model can be developed for a wider range of applications, including assisting individuals with hand disabilities. Such an enhancement will not only expand the scope of potential applications, but will also contribute significantly to the development of assistive technologies for individuals with physical impairments.

## REFERENCES

- [1] E. Y. Y. Chan *et al.*, "Reflection of Challenges and Opportunities within the COVID-19 Pandemic to Include Biological Hazards into DRR Planning," *International Journal of Environmental Research and Public Health*, vol. 18, no. 4, Feb. 2021, Art. no. 1614, <https://doi.org/10.3390/ijerph18041614>.
- [2] W. R. Keatinge, S. R. K. Coleshaw, J. C. Easton, F. Cotter, M. B. Mattock, and R. Chelliah, "Increased platelet and red cell counts, blood viscosity, and plasma cholesterol levels during heat stress, and mortality from coronary and cerebral thrombosis," *The American Journal of*

- Medicine*, vol. 81, no. 5, pp. 795–800, Nov. 1986, [https://doi.org/10.1016/0002-9343\(86\)90348-7](https://doi.org/10.1016/0002-9343(86)90348-7).
- [3] D. Vecchio, A. J. Saso, and C. I. Cann, "Occupational risk in health care and research," *American Journal of Industrial Medicine*, vol. 43, no. 4, pp. 369–397, Apr. 2003, <https://doi.org/10.1002/ajim.10191>.
- [4] V. Leso, M. L. Ercolano, D. L. Cioffi, and I. Iavicoli, "Occupational Chemical Exposure and Breast Cancer Risk According to Hormone Receptor Status: A Systematic Review," *Cancers*, vol. 11, no. 12, Nov. 2019, Art. no. 1882, <https://doi.org/10.3390/cancers11121882>.
- [5] J. L. Stewart-Evans, A. Sharman, and J. Isaac, "A narrative review of secondary hazards in hospitals from cases of chemical self-poisoning and chemical exposure," *European Journal of Emergency Medicine: Official Journal of the European Society for Emergency Medicine*, vol. 20, no. 5, pp. 304–309, Oct. 2013, <https://doi.org/10.1097/MEJ.0b013e32835d002c>.
- [6] L. E. Sánchez-Velasco, M. Arias-Montiel, E. Guzmán-Ramírez, and E. Lugo-González, "A Low-Cost EMG-Controlled Anthropomorphic Robotic Hand for Power and Precision Grasp," *Biocybernetics and Biomedical Engineering*, vol. 40, no. 1, pp. 221–237, Jan. 2020, <https://doi.org/10.1016/j.bbe.2019.10.002>.
- [7] N. Naseer, F. Ali, S. Ahmed, S. Iftikhar, R. A. Khan, and H. Nazeer, "EMG Based Control of Individual Fingers of Robotic Hand," in *2018 International Conference on Sustainable Information Engineering and Technology (SIET)*, Malang, Indonesia, Nov. 2018, pp. 6–9, <https://doi.org/10.1109/SIET.2018.8693177>.
- [8] N.-K. Nguyen, T.-M.-P. Dao, T.-D. Nguyen, D.-T. Nguyen, H.-T. Nguyen, and V.-K. Nguyen, "An sEMG Signal-based Robotic Arm for Rehabilitation applying Fuzzy Logic," *Engineering, Technology & Applied Science Research*, vol. 14, no. 3, pp. 14287–14294, Jun. 2024, <https://doi.org/10.48084/etasr.7146>.
- [9] Y. Yamakawa, Y. Katsuki, Y. Watanabe, and M. Ishikawa, "Development of a High-Speed, Low-Latency Telemanipulated Robot Hand System," *Robotics*, vol. 10, no. 1, Mar. 2021, Art. no. 41, <https://doi.org/10.3390/robotics10010041>.
- [10] S. Latif, J. Javed, M. Ghafoor, M. Moazzam, and A. A. Khan, "Design and development of muscle and flex sensor controlled robotic hand for disabled persons," in *2019 International Conference on Applied and Engineering Mathematics (ICAEM)*, Taxila, Pakistan, Aug. 2019, pp. 1–6, <https://doi.org/10.1109/ICAEM.2019.8853757>.
- [11] J. D. Setiawan, M. Ariyanto, M. Munadi, M. Mutoha, A. Glowacz, and W. Caesarendra, "Grasp Posture Control of Wearable Extra Robotic Fingers with Flex Sensors Based on Neural Network," *Electronics*, vol. 9, no. 6, Jun. 2020, Art. no. 905, <https://doi.org/10.3390/electronics9060905>.
- [12] P. Weber, E. Rueckert, R. Calandra, J. Peters, and P. Beckerle, "A low-cost sensor glove with vibrotactile feedback and multiple finger joint and hand motion sensing for human-robot interaction," in *2016 25th IEEE International Symposium on Robot and Human Interactive Communication (RO-MAN)*, New York, NY, USA, Aug. 2016, pp. 99–104, <https://doi.org/10.1109/ROMAN.2016.7745096>.
- [13] A. H. Zaidan, M. K. Wail, and A. A. Yaseen, "Design and Implementation of Upper Prosthetic Controlled remotely by Flexible Sensor Glove," *IOP Conference Series: Materials Science and Engineering*, vol. 1105, no. 1, Jun. 2021, Art. no. 012080, <https://doi.org/10.1088/1757-899X/1105/1/012080>.
- [14] S. Bilgin, Y. User, and M. Mercan, "Robotic Hand Controlling Based on Flexible Sensor," *International Journal Of Engineering & Applied Sciences*, vol. 8, pp. 49–49, Dec. 2016, <https://doi.org/10.24107/ijeas.281463>.
- [15] S. Z. Ying, N. K. Al-Shammari, A. A. Faudzi, and Y. Sabzehmeidani, "Continuous Progressive Actuator Robot for Hand Rehabilitation," *Engineering, Technology & Applied Science Research*, vol. 10, no. 1, pp. 5276–5280, Feb. 2020, <https://doi.org/10.48084/etasr.3212>.
- [16] H. G. Doan and N. T. Nguyen, "Fusion Machine Learning Strategies for Multi-modal Sensor-based Hand Gesture Recognition," *Engineering, Technology & Applied Science Research*, vol. 12, no. 3, pp. 8628–8633, Jun. 2022, <https://doi.org/10.48084/etasr.4913>.
- [17] M. M. Al-Zu'bi, M. A. Khodeir, and M. F. Al-Mistarihi, "Modeling and design of an infrared-based identification (IRID) system-tag and reader design," in *2014 5th International Conference on Information and Communication Systems (ICICS)*, Irbid, Jordan, Apr. 2014, pp. 1–5, <https://doi.org/10.1109/IACS.2014.6841967>.
- [18] P. Dhepekar and Y. G. Adhav, "Wireless robotic hand for remote operations using flex sensor," in *2016 International Conference on Automatic Control and Dynamic Optimization Techniques (ICACDOT)*, Pune, India, Sep. 2016, pp. 114–118, <https://doi.org/10.1109/ICACDOT.2016.7877562>.
- [19] Azhari, T. I. Nasution, S. H. Sinaga, and Sudiati, "Design of Monitoring System Temperature And Humidity Using DHT22 Sensor and NRF24L01 Based on Arduino," *Journal of Physics: Conference Series*, vol. 2421, no. 1, Jan. 2023, Art. no. 012018, <https://doi.org/10.1088/1742-6596/2421/1/012018>.
- [20] W. Setya *et al.*, "Design and development of measurement of measuring light resistance using Light Dependent Resistance (LDR) sensors," *Journal of Physics: Conference Series*, vol. 1402, no. 4, Dec. 2019, Art. no. 044102, <https://doi.org/10.1088/1742-6596/1402/4/044102>.
- [21] Z. Yao-lin, Z. Gao-qiang, Z. Lei, and X. Jin, "Design of wireless multi-point temperature transmission system based on nRF24L01," in *2011 International Conference on Business Management and Electronic Information*, Guangzhou, China, May 2011, vol. 3, pp. 780–783, <https://doi.org/10.1109/ICBMEI.2011.5920375>.
- [22] B. Micó-Vicent, E. Perales, K. Huraibat, F. M. Martínez-Verdú, and V. Viqueira, "Maximization of FDM-3D-Objects Gonio-Appearance Effects Using PLA and ABS Filaments and Combining Several Printing Parameters: 'A Case Study,'" *Materials*, vol. 12, no. 9, Jan. 2019, Art. no. 1423, <https://doi.org/10.3390/ma12091423>.